Nanoscale

MINIREVIEW

View Article Online
View Journal | View Issue

Check for updates

Cite this: *Nanoscale*, 2024, **16**, 2789

Organic nanomotors: emerging versatile nanobots

Jingjun Jin,†[a] Yan Li,†[a] Shuai Wang,*[b] Jianchun Xie*[c] and Xibo Yan *[a]

Received 25th November 2023,
Accepted 29th December 2023

DOI: 10.1039/d3nr05995b

rsc.li/nanoscale

Artificial nanomotors are self-propelled nanometer-scaled machines that are capable of converting external energy into mechanical motion. A significant progress on artificial nanomotors over the last decades has unlocked the potential of carrying out manipulatable transport and cargo delivery missions with enhanced efficiencies owing to their stimulus-responsive autonomous movement in various complex environments, allowing for future advances in a large range of applications. Emergent kinetic systems with programmable energy-converting mechanisms that are capable of powering the nanomotors are attracting increasing attention. This review highlights the most-recent representative examples of synthetic organic nanomotors having self-propelled motion exclusively powered by organic molecule- or their aggregate-based kinetic systems. The stimulus-responsive propulsion mechanism, motion behaviors, and performance in antitumor therapy of organic nanomotors developed so far are illustrated. A future perspective on the development of organic nanomotors is also proposed. With continuous innovation, it is believed that the scope and possible achievements in practical applications of organic nanomotors with diversified organic kinetic systems will expand.

Published on 02 ianuarie 2024. Downloaded on 04.01.2026 05:56:20.

1. Introduction

Nanomotors are tiny artificial devices that translate external energy (chemical,[1] light,[2] ultrasound,[3] magnetic,[4] *etc.*) into mechanical motion in liquid media.[5–7] This stimulus-responsive autonomous movement can effectively strengthen nanomaterials in carrying out various sophisticated missions in the microenvironment, including drug delivery,[8] sensing,[9] imaging,[10] and environmental remediation.[11] These intelligent nanomachines mainly rely on chemically or physically responsive components installed within nanoparticles that would work as kinetic systems for efficient energy conversion.[12,13] Meanwhile, the inherent anisotropic nature of colloid morphologies/shapes facilitates the creation of asymmetric energy gradients across nanoparticles in response to external stimuli, which provides the driving force for powering a self-propelled motion.[14–17] In the past decades, considerable efforts have been contributed to the design and development of advanced kinetic systems of these nanoscale vehicles for the programmable manipulation and precise modulation of mechanical work, particularly while considering the integration of these nanomotors into a large variety of applications.[18–20] Since the first model of catalytic nanomotors comprising platinum and gold segments was reported in 2004,[21] inorganic metals, owing to their diverse and excellent energy-converting behaviors, have become the most widely applied kinetic engines to power self-propulsion in liquid media.[22] Some energy transfer processes (*e.g.* chem-/photo-catalytic reactions and photothermal conversions) can simultaneously improve material performance.[23–25] However, the potential safety issues of these undegradable

[a]*School of Chemical Engineering and Technology, Tianjin University, Tianjin, 300072, China. E-mail: xiboyan@tju.edu.cn*
[b]*College of Food Science and Engineering, Tianjin University of Science and Technology, Tianjin, 300457, China. E-mail: wangshuai@tust.edu.cn*
[c]*China Food Flavor and Nutrition Health Innovation Center, Beijing Technology and Business University, Beijing100048, China. E-mail: xjchun@th.btbu.edu.cn*
†These authors contributed equally to this manuscript.

Xibo Yan

Dr Xibo Yan received his B.E. degree from Tianjin University and his M.S. degree from Nankai University. He completed his Ph.D. research under the guidance of Prof. Etienne Fleury from INSA de Lyon in 2015. After working as a post-doctoral researcher at Laboratoire Ingénierie des Matériaux Polymères (Lyon) with Dr François Ganachaud and Dr Julien Bernard for three years, he began his independent career as an associate professor at Tianjin University in 2019. His research interests include intelligent polymeric nanomaterials, polymer self-assembly, and biomacromolecules.

Published on 02 ianuarie 2024. Downloaded on 04.01.2026 05:56:20.

engineered nanomaterials on the environment and health are always a concern. Particularly in biomedical fields, heavy metal-based nanoparticles could give rise to the risks of damaging cellular membranes *via* electrostatic or hydrophobic interactions[26,27] and causing long-term and non-specific toxicity.[28–30] Hence, the biosafety of these nanoparticles should be considered and addressed for practical applications.

Nowadays, organic nanomaterials have been widely used as controlled drug delivery systems owing to their good biocompatibility.[31] Generally, these multifunctional nanoparticles capable of carrying therapeutic and diagnostic agents are engineered to passively navigate in complex *in vitro* and *in vivo* environments. These organic nanocarriers can also be ideal supporting architectures for attaching or encapsulating metal-based kinetic engines for the effective improvement of their biocompatibility.[32] Meanwhile, with the recent progress of nanotechnologies in molecular assembly and nanofabrication, although the construction of artificial nanomotors with complex compositions and structures is always greatly challenging,[33,34] completely-organic nanomotors fabricated from a variety of organic substrates (including small molecules or/and polymers) with biocompatibility and biodegradability have been developed and have attracted increasing attention. In stark contrast to conventional nanomotors, recent research has shown that the organic components themselves could work as stimulus-responsive energy-converting systems (engines or fuels) for powering the propulsion. Synthetic organic small molecules and/or polymers with great flexibility in structures, properties, and functions allow on-demand programming of energy-converting manners to regulate the motile features of the nanomotors for adapting to various sophisticated applications. Thanks to that, these organic kinetic systems enable driving the nanomotors with excellent biocompatibility and controllability, and some of their energy conversion processes can also effectively modulate the physiological environments and even perform therapeutics against lesions with highly precise manipulability. Besides, bio-sourced enzymes (*e.g.*, catalase, urease, and glucose oxidase) with high substrate specificity are regarded as one kind of biocompatible organic engine for powering catalytic propulsion, which has been exhaustively reviewed in the last decade.[34–37] In this review, we focus on recent advances in developing organic nanomotors with stimulus-responsive synthetic organic molecules or their aggregates made kinetic systems and highlight the corresponding propulsion mechanisms with classification according to their energy-converting behaviors. In addition, the potential applications of these intelligent organic nanomachines in antitumor therapy are presented and discussed. A summary and an outlook of prospects are also provided in the last section.

2. The motion principle of organic nanomotors

The kinetic systems of organic nanomotors are fabricated from a variety of stimulus-responsive synthetic organic molecules or their aggregates, which would undergo catalytic degradation reactions (working as fuels) or perform energy-converting processes (working as engines) for powering the self-propelled movement in aqueous solution or biomimetic environments (Fig. 1). Besides, a new generation of nanomotors with organic kinetic systems of integrating multiple stimulus-responsive behaviors has been recently developed. Taking advantage of the versatility of synthetic organic molecules in molecule construction and energy transition would achieve the programming of multiple energy gradients for further reinforcing mobility.

2.1. Organic molecules as consumable fuels

Synthetic organic molecules can work as consumed fuels loaded into the nanoparticles by physical encapsulation or chemical incorporation. In response to various external stimuli (light, enzyme, *etc.*), these organic fuels can carry out controllable catalytic degradation to gradually produce and release small molecule chemicals to the surrounding medium, creating a chemical gradient across the particles, which would spontaneously exert the diffusiophoresis force on the nanomotors for powering self-diffusiophoresis in the liquid media.

2.1.1 N_2-driven organic nanomotors. Nitrogen is abundant in the atmosphere and has been considered and utilized as an inert gas in many fields. Azo-based molecules are well-known radical initiators that can produce nitrogen gas through light or temperature-triggered dissociation.[38,39] Landfester and Crespy reported on the preparation of 2,2′-azobis (2-methylpropionitrile) (AIBN)-loaded silica-based asymmetric nanocapsules with a diameter of ~100 nm *via* a one-pot confined sol–gel process at the oil/water interface of miniemulsion droplets (Fig. 2A).[40] The ^{1}H NMR spectra confirmed the loading of AIBN in the nanoparticles with a concentration of 1.48 mg mL^{-1}. UV irradiation and heating can rapidly decompose the AIBN with first-order kinetics in the inner cavity of the particles for the controlled release of nitrogen gas to the liquid medium, which made AIBN become light- or thermo-responsive fuels for powering the nanoparticles to perform autonomous movement in the solution. Compared with Brownian motion, an increase in the effective diffusion coefficient (ΔD_{eff}) of thermodriven propulsion can go up to 3 μm^2 s^{-1} (80 °C).

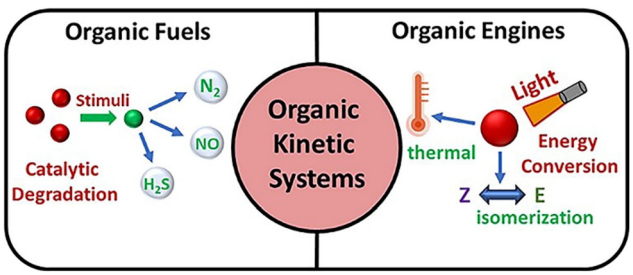

Fig. 1 Illustrated summary of stimulus-responsive organic kinetic systems for powering organic nanomotors.

This journal is © The Royal Society of Chemistry 2024

Published on 02 ianuarie 2024. Downloaded on 04.01.2026 05:56:20.

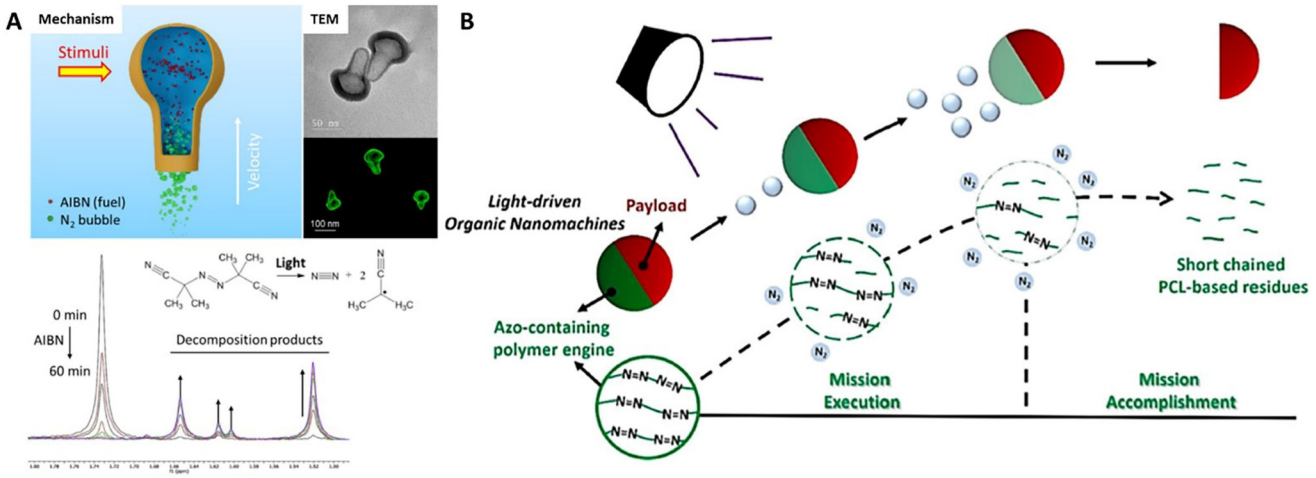

Fig. 2 Organic nanomotors with azo-based organic fuels. (A) Photo-/temperature-responsive AIBN-loaded N_2-driven nanomotors.[40] Reproduced from ref. 40 with permission from American Chemical Society, copyright 2020. (B) Photoresponsive N_2-driven azo-containing polyurethane-based nanomotors.[41] Reproduced from ref. 41 with permission from Elsevier Ltd, copyright 2022.

In addition to azo-based small molecules, Feng *et al.* synthesized azo-containing polyurethane *via* a classic polycondensation of dihydroxy-poly(ε-caprolactone), hexamethylene diisocyanate, and 2,2′-azobis(2-methyl-*N*-(2-hydroxyethyl)propionamide) (12.5 mol% of azo-moieties along the polymer backbone).[41] The azo-containing polymers can be self-assembled with biodegradable polypeptide (poly(γ-benzyl-L-glutamate), PBLG) or macromolecular prodrug (camptothecin (CPT)-bearing methacrylate-based copolymers) into asymmetric nanoparticles with a diameter of 165 nm through a scalable continuous nanoprecipitation by rapidly mixing water stream and THF stream in a multi-inlet vortex mixer. In response to UV irradiation, azo-linkages within the polymer chains underwent gradual decomposition for nitrogen generation, which allowed simultaneously achieving a light-response nitrogen release and polymer degradation (Fig. 2B). This effectively powered the polymer colloids for carrying out the delivery mission with ultrafast propulsion in a large range of aqueous solution (water, PBS buffer, high viscous sugar solution) and biological environments (extracellular matrix); the maximal velocities can reach ~150 μm s^{-1}. Meanwhile, the azo-containing polymer phase within the nanoparticles can be gradually degraded with irradiation, resulting in complete nanostructure dissociation after mission accomplishment, which would relieve the potential risks of engineered nanomaterials to the environment and health.

2.1.2 NO-driven organic nanomotors. Nitric oxide is one of most important signalling molecules or effectors in various bio-regulatory systems.[42,43] In mammalian cells, an L-arginine-NO metabolic pathway can convert L-arginine into NO molecules by nitric oxide synthetases (NOS) or reactive oxygens (ROS).[44,45] Inspired by these endogenous biochemical reactions, Shen and Mao designed and fabricated nitric oxide-driven nanomotors by incorporating L-arginine into hyperbranched polyamide-based nanoparticles *via* electrostatic attraction (Fig. 3A).[46] In response to H_2O_2 (ROS), L-arginine at the surface of nanoparticles was progressively consumed to convert into NO bubbles in the solution, which would effectively power the nanoparticles for self-propulsion in the aqueous solution and biological environment of MCF-7 cells. The particle velocities were increased with the amount of L-arginine within the particles and the concentration of H_2O_2 in the surrounding medium. Thanks to the convenient non-covalent functionalization process, L-arginine can also be incorporated or encapsulated into bowl-shaped mesoporous silica nanoparticles,[47] poly-carboxybetaine methacrylate nanoparticles,[48] and heparin/folic acid nanoparticles[49,50] to work as bio-responsive self-degradable fuels for powering the autonomous motion. Meanwhile, zwitterionic L-arginine can also work as a functional substrate to prepare a series of methacrylate- or trehalose-functionalized L-arginine,[51–54] which would be further self-assembled into L-arginine-fueled organic nanoparticles with NO-driven propulsion in the complex biological environments.

Besides, NO donors are one kind of synthetic organic compounds, which can be transformed into NO *in vitro* and *in vivo via* various enzymatic- or chemical-reactions.[55] Thanks to the structural diversity of NO donors, the stimulus-responsive NO production can be conveniently modulated to meet the demand of various biomedical applications,[56–58] such as anti-inflammatory treatment, cardiovascular therapy, and anti-cancer treatment. To achieve stable NO production, Li and co-workers directly grafted thiolated NO donors onto the pre-formed Fe_3O_4-based Janus nanoparticles to form NO-driven hybrid nanomotors with a diameter of 233 nm (Fig. 3B).[59] In response to glutathione (GSH) in the surrounding medium, thanks to the asymmetric distribution of NO donors at the surface of particles, NO would be produced and released from one side of particles, which can power the self-diffusiophoresis in the aqueous solution with a velocity of 7.60 μm s^{-1} and the network of chitosan gel with a velocity of 3.14 μm s^{-1}.

Published on 02 ianuarie 2024. Downloaded on 04.01.2026 05:56:20.

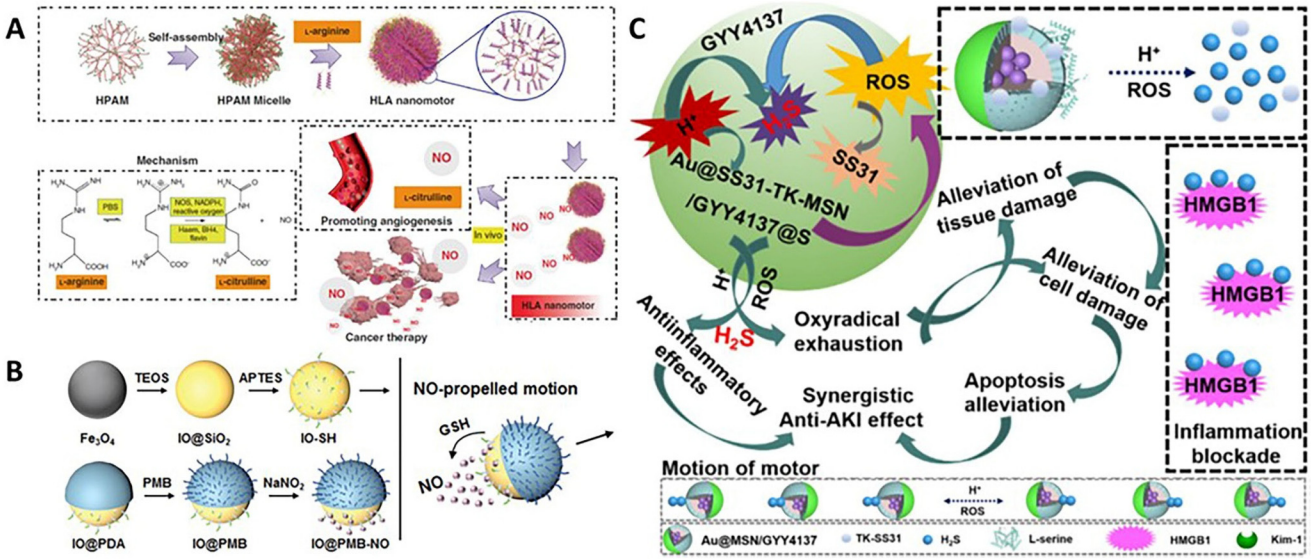

Fig. 3 Organic nanomotors with bio-responsive organic fuels. (A) Enzyme/ROS-responsive NO-driven nanomotors.[46] Reproduced from ref. 46 with permission from Springer Nature Limited, copyright 2019. (B) GSH-responsive NO-driven nanomotors.[59] Reproduced from ref. 59 with permission from The Royal Society of Chemistry, copyright 2022. (C) H^+/ROS-responsive H_2S-driven nanomotors.[65] Reproduced from ref. 65 with permission from Royal Society of Chemistry, copyright 2023.

2.1.3 H_2S-driven organic nanomotors. Hydrogen sulfide (H_2S) is one of the important physiological active molecules in the human body.[60] The exogenous H_2S can promote the cellular uptake of glucose and inhibit the efflux of protons.[61] L-cysteine can be catalyzed by cystathionine β-synthase (highly expressed in the tumor microenvironment) to generate H_2S and L-serine.[62] To construct H_2S-driven nanomotors, Wan and co-workers firstly prepared zwitterion-based nanoparticles with a size of 200 nm by the free radical polymerization of zwitterionic sulfobetaine methacrylate and *N*,*N*′-bis-(acryloyl) cystamine.[63] L-cysteine as enzyme-responsive fuels was post-loaded by co-incubation with nanoparticles. The polymeric nanoparticles can be degraded in response to glutathione in tumors. Compared with incubation with normal cells, the colloidal motors showed much higher H_2S production in the environment of cancer cells, resulting in a much faster self-diffusiophoresis (velocity: 5–6 μm s^{-1}). The results confirmed the significant contribution of cystathionine β-synthase-catalyzed H_2S production to autonomous movement.

(*p*-Methoxyphenyl)morpholino-phosphinodithioic acid (GYY4137) is another important H_2S donor capable of releasing H_2S in physiological environment.[64] The release rates can be effectively increased in the acidic condition. Tong *et al.* prepared GYY4137-loaded mesoporous silica-based nanoparticles with the asymmetric decoration of gold nanoparticles, which can be used as pH-activated nanomotors for carrying out the mission in a low-pH environment (Fig. 3C).[65] H_2S release from these asymmetric nanoparticles with a size of 73 nm (determined by TEM) was significantly increased in pH 5.0 PBS with 10 mM H_2O_2. Hence, GYY4137 can be regarded as pH-responsive organic fuels for powering colloidal motors. Compared with Brownian motion in pH 7.4 PBS, the nanomotors showed pH-triggered self-propulsion in pH 5.0 PBS with 10 mM H_2O_2; the velocity can go up to 4.62 μm s^{-1}.

2.2. Organic molecules as energy converting engines

The synthetic organic molecules or their aggregates can work as kinetic engines installed on the nanoparticles, which are of very high stability in structures, properties, and functions during energy conversion. Light is the most widely applied external stimuli to activate these types of organic engines. In general, the photoresponsive energy conversion within the nanomotors independent of the surrounding chemical medium can spontaneously produce energy (surface tension, thermal, *etc.*) gradients in the vicinity of the particles. According to the nature of energy gradients, the organic engines exposed to light could provide the corresponding driving force for powering the nanomotors for self-thermophoresis or self-diffusiophoresis in the liquid media.

2.2.1. Photoisomerization-driven organic nanomotors. Photochromic materials can perform a reversible molecular transformation in response to light irradiation, which would lead to an effective shifting of the physicochemical properties of the materials.[66,67] Particularly, the photoisomerization of azobenzene-based materials can induce surface-free energy switching between *trans*-form (low energy) and *cis*-form (high energy) to create surface tension gradients at the surface, which has been widely utilized in the investigation of the light-driven motion of polymer particles and water droplets on the azobenzene-containing surface.[68,69] Besides, azobenzene moieties grafted onto the nanomotors with mono- or multiple porosities can be used as photoactivated switches capable of regulating the chemical release manners from the internal cavity of the particles *via* host–guest interactions, resulting in the light-

 This journal is © The Royal Society of Chemistry 2024

Published on 02 ianuarie 2024. Downloaded on 04.01.2026 05:56:20.

driven control of particle locomotion.[70,71] In contrast, Abid *et al.* directly grafted a large number of azobenzene-based moieties (270 azobenzene per particle) on the surface of preformed polystyrene nanoparticles *via* covalent bonds to generate 16 nm-scaled light-driven nanomotors (Fig. 4A).[72] In response to 473 nm irradiation, the photoisomerization of azobenzene moieties at the surface of particles would convert light into sufficient mechanical work to propel the particle with optical control by light intensity gradients. The maximal velocities can go up to 15 μm s^{-1} in the aqueous solution of 10 or 15 wt% of poly(vinyl alcohol) (100 W cm^{-2}). The particle motion analysis confirmed that photoisomerization would be the main driving force powering the self-propulsion rather than the optical force. Also, the photochromic spiropyran was used to functionalize hyperbranched polymer Boltorn H40, which could form micro-scaled organic colloids in water/dimethylsulfoxide (1/5, v/v).[73] Under asymmetric UV irradiation, the photoisomerization of siropyran moieties induced a surface tension gradient across the particles, which could exert a propulsive force on the particles to effectively power the autonomous motion in the aqueous solution. These interesting photoresponsive behaviors endowed particle locomotion with a good sensibility to the direction and gradient light fields, showing an obvious phototactic orientation.

2.2.2. Photothermal-driven organic nanomotors. Photothermal nanoparticles can strongly absorb light energy and convert it into heat *via* electron–phonon coupling, which could transfer from nanoparticles to the surrounding medium for a temperature increase. Also, an asymmetric thermal distribution across the particle can be used as the driving force for self-thermophoresis (photothermal propulsion).[74] Recently, except from plasmonic metal components,[75] various organic chromophore aggregates also exhibit good non-radiative light-to-heat conversion in the energy dissipation of the chromophores after excitation.[76] Some of them have been successfully developed as photothermal engines for nanomotor fabrication.

Indocyanine green (ICG) is a cyanine fluorescent dye with strong absorption in the near-infrared region.[77,78] Thanks to the great biocompatibility, ICG has been approved by United States Food and Drug Administration in 1954 for diagnostic applications. Nowadays, ICG capable of converting NIR light into thermal and reactive oxygen species are widely applied in photothermal and/or photodynamic therapy. Recently, Tu and Peng reported on photoactivated ICG/DOX-dual drug-loaded nanomotors with a calabash-like morphology (Fig. 4B).[79] Their symmetric counterpart within one particle was formed *via* a double emulsion solvent evaporation technique, which also allowed the co-encapsulation of hydrophilic (ICG) and hydrophobic (DOX) drugs in the particles with a diameter of ~120 nm. The light-responsive ICG molecules were trapped in the PCL/PLGA polymer phase at one side of the particles, conferring the particles with a laser power-dependent photothermal converting capability under 808 nm NIR irradiation (laser

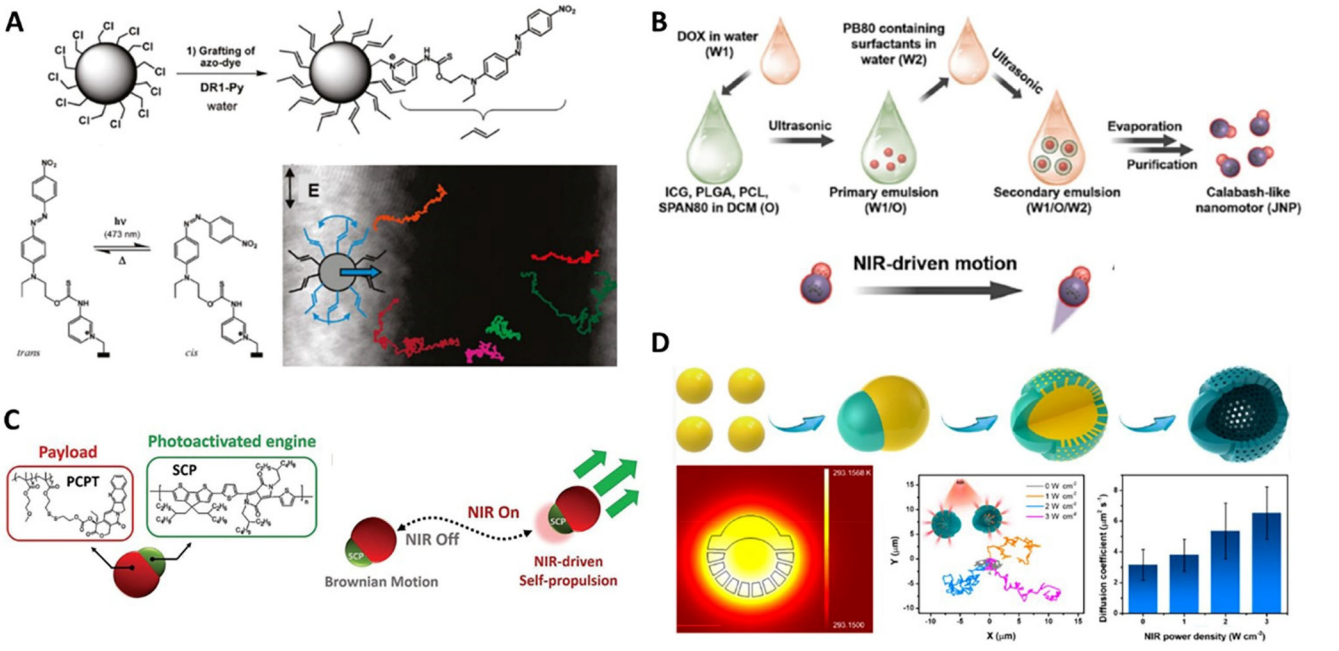

Fig. 4 Organic nanomotors with organic energy-converting engines. (A) Photoisomerization-driven organic nanomotors with visible light-responsive azobenzene-based engines.[72] Reproduced from ref. 72 with permission from American Chemical Society, copyright 2011. (B) Photothermal-driven organic nanomotors with NIR-responsive ICG-based engines.[79] Reproduced from ref. 79 with permission from Elsevier Ltd, copyright 2023. (C) Photothermal-driven organic nanomotors with NIR-responsive semiconducting conjugated polymer-based engines.[83] Reproduced from ref. 83 with permission from Wiley-VCH GmbH, copyright 2022. (D) Photothermal-driven organic nanomotors with NIR-responsive carbon-based engines.[88] Reproduced from ref. 88 with permission from American Chemical Society, Copyright 2022.

Published on 02 ianuarie 2024. Downloaded on 04.01.2026 05:56:20.

power: 0–20 W cm^{-2}). Thanks to the asymmetric distribution of ICG within the nanomotors, the NIR-responsive photothermal conversion that occurred within PCL/PLGA polymer phases would create an asymmetric thermal gradient across the particles for powering the thermophoresis from hot to cold region in the complex biological environment in the presence of the glioma cell GL261. In contrast, Zhang *et al.* encapsulated ICG derivatives and DOX into the mesoporous silica nanoparticles to construct a photoresponsive symmetric nanoparticles with a diameter of 189 nm.[80] The photothermal ICG derivatives would also work as light-to-heat converting components to support the light-driven motion in the solution with various pH (5.5, 6.5, and 7.4), and the maximal velocities (16.1 μm s^{-1}) were obtained in the pH 5.5 solution under 808 nm irradiation with a laser power of 1.5 W cm^{-2}, which may be attributed to additional heat produced by the accelerated release of DOX in the acidic solution.

Semiconducting π-conjugated polymers (SCP)-based nanoparticles with excellent photostability and tunable optical properties have become one of the most competent nanoagents in NIR fluorescence imaging, photoacoustic imaging, photothermal, and/or photodynamic therapy.[81,82] In contrast to metal nanoparticles, the photophysical properties of SCP-based nanoparticles are less dependent on their sizes. The photothermal conversion efficiencies are mainly determined by the electron donor–acceptor backbone structures. Recently, we reported on the straightforward fabrication of asymmetric polymer colloidal motors assembled by semiconducting conjugated polymers and macromolecular anticancer prodrugs *via* a classic nanoprecipitation process (Fig. 4C).[83] The 145 nm-scaled SCP-based nanoparticles with a broad absorption from visible light to NIR wavelength can perform a stable photothermal converting behavior in response to 808 nm NIR irradiation with various laser powers (0–2 W cm^{-2}). In this case, the asymmetric presence of SCP phases within the particles can be used as NIR-fueled engines to power photoactivated thermophoresis for facilitating macromolecular prodrug (camptothecin-bearing methacrylate-based copolymers) delivery. The particle locomotion would be accelerated with laser powers and irradiation time; the maximal velocities can reach 100 μm s^{-1} after long-termed irradiation (1 W cm^{-2}).

Polydopamine (PDA)-based nanoparticles with similar structures to natural melanin have shown good biocompatibility in biomedical applications.[84] Also, strong NIR absorption and high light-to-heat converting capability makes them good candidates for photothermal therapy. Zhao and coworkers prepared NIR-driven methoxy polyethylene glycol-functionalized walnut-shaped PDA nanomotors with a diameter of 353 nm.[85] The resulting nanoparticles showed a good photothermal conversion efficiency (around 40%). Under 808 nm laser irradiation, the walnut-shaped colloidal motors enabled photoactivated autonomous movement in the MCF-7 cell culture. The particle velocities were increased with the laser power, reaching 4.72 μm s^{-1} using a laser power of 2 W cm^{-2}. In addition to powering self-thermophoresis, the presence of PDA nanoparticles within the colloidal motors under NIR irradiation can also facilitate the performance of enzymatic catalytic self-diffusiophoresis for significantly enhancing the diffusion coefficient in the liquid media.[86]

Besides, carbon nanomaterials with excellent light-absorption toward broad wavelengths are also one of the most practical photothermal nano-agents in photothermal therapy.[87] Kong and coworkers precisely fabricated jellyfish-like asymmetric porous hollow carbon nanoparticles through a kinetic-controlled interfacial super-assembly process using silica nanoparticles as sacrificial precursors (Fig. 4D).[88] The porous nanoparticles showed a very broad and strong light-absorption form visible to NIR light, and the maximal absorption wavelength was about ~970 nm. Under 980 nm laser irradiation, the carbon nanoparticles performed a rapid light-to-heat conversion with the laser powers and concentration dependent-behaviors. In this case, the asymmetric photothermal conversion can effectively power the nanoparticles for light-driven self-propulsion in the solution. A significant increase in the diffusion coefficient of nanoobjects was observed, it could go up to 6.54 μm^2 s^{-1} in response to 980 nm irradiation with a laser power of 3 W cm^{-2}, confirming the autonomous movement overcoming Brownian motion.

2.3. Organic molecules as multi-mode kinetic systems

Currently, most nanomotors are powered by kinetic systems with a single energy-converting mode. Meanwhile, recent studies have exhibited a new generation of hybrid nanomotors with multimode propulsion by installing multi-responsive kinetic systems,[13] which could significantly improve the precision of manipulating and modulating such tiny nanobots in the complex microenvironment. In addition, some multimode organic kinetic systems have also been developed for powering self-propulsion combining multiple motion mechanisms. This would confer the nanomotors with enhanced motile performance for effectively expanding the potential of organic nanomotors in practical applications.

2.3.1. Photothermal/catalytic-driven organic nanomotors. Among all the energy-converting manners, photothermal- and catalytic-powered self-propulsion are the most popular motile mode for manipulating the nanomotors in the microenvironment. The organic nanomotors with multimode propulsion can be conveniently reinforced by constructing the kinetic systems combining two motile mechanisms. Depending on the nature of the catalytic reaction involved, photothermal/chem-catalytic, photothermal/thermocatalytic, and photothermal/photocatalytic organic nanomotors have been developed.

Photothermal/chem-catalytic kinetic system. NO-driven nanomotors have shown good motile performance in the liquid media and biological environments. To further reinforce this amino acid-fueled nanomaterials for multimode propulsion, initially, L-arginine and photoresponsive gold nanoparticles were used to functionalize the β-cyclodextrin-based organic nanoparticles, which enabled performing photothermal conversion and ROS-responsive NO production in the environment of RAW264.7 cells under 808 nm NIR irradiation (2.5 W cm^{-2}).[89] Simultaneous energy conversion within the particles

 This journal is © The Royal Society of Chemistry 2024

Published on 02 ianuarie 2024. Downloaded on 04.01.2026 05:56:20.

can lead to photothermal/chem-catalytic dual-mode synergistic propulsion, showing much faster locomotion than single-mode one (NIR or ROS). Also, Mao and Wan functionalized photothermal bowl-like porous polydopamine nanoparticles with L-arginine-containing RGD peptides to construct 200 nm-scaled completely organic dual-responsive colloidal motors (Fig. 5A).[90] Similarly, 808 NIR irradiation and ROS can simultaneously trigger energy conversion for facilitating dual-mode propulsion in biological environments. In addition, the same group incorporated L-arginine and ICG into biocompatible poly(2-methacryloyloxyethyl phosphorylcholine-s-s-vinylimidazole)-based nanogels to form submicron dual-responsive nanomotors (Fig. 5B).[91] For this system, ROS can be self-produced by ICG molecules within the particles in response to 808 nm NIR irradiation. In this case, the NIR irradiation firstly triggered a classic photothermal conversion of ICG and simultaneously generated ROS, which would sequentially induce the NO production *via* ROS-responsive L-arginine-NO reaction for powering dual-mode synergistic propulsion with a velocity of 5.6 μm s^{-1} (808 nm, 1 W cm^{-2}). In contrast to general NO-driven nanomotors whose motile features are limited to the surrounding ROS level, these unique photoactivated ROS-self-produced nanomaterials can achieve stable autonomous motion independent of surrounding media, which could be applied to carry out sophisticated missions in various microenvironments.

Photothermal/thermocatalytic kinetic system. In addition to photothermal conversion, some thermoresponsive organic reactions can be simultaneously introduced to program sequential energy transition within the colloidal motors for further reinforcing the particle mobility. For instance, the thermoresponsive acyl azide groups can be incorporated into macromolecular prodrugs (camptothecin-bearing methacrylate-based copolymers) by polymerization and post-functionalization, which could further self-assemble with semiconducting conjugated polymers for constructing asymmetric organic nanorockets with a diameter of 105 nm (Fig. 5C).[92] Thanks to the presence of acyl azides within the particles, the artificial colloidal motors can undergo a classic Curtius rearrangement in response to the physiological temperature (37 °C) to release nitrogen for thermodriven self-diffusiophoresis. More interestingly, 808 nm NIR irradiation with tunable laser powers (0–2 W cm^{-2}) can initially trigger the photothermal conversion within SCP phases, and the correspondingly produced thermal energy would sequentially induce the Curtius rearrangement reaction within acyl azide-based phases to robustly push nitrogen out to the surrounding media. Such a two-stage light-to-heat-to-chemical energy transition would effectively power the organic nanorockets for a light-driven ultrafast self-propulsion (up to 300 μm s^{-1}) in the solution.

Photothermal/photocatalytic kinetic system. Although multi-mode propulsion can significantly strengthen the propulsion under the regulation of multiple energy sources, the on-demand installation of multiple stimulus-responsive components onto the nanomaterials generally relies on a series of time-intensive assembly processes. Also, the introduction of multiple energy sources with diverse operations, intensities, and orientations would seriously complicate the manipulation and modulation of particle locomotion. Moreover, it is very difficult to make multiple energy inputs with the complete

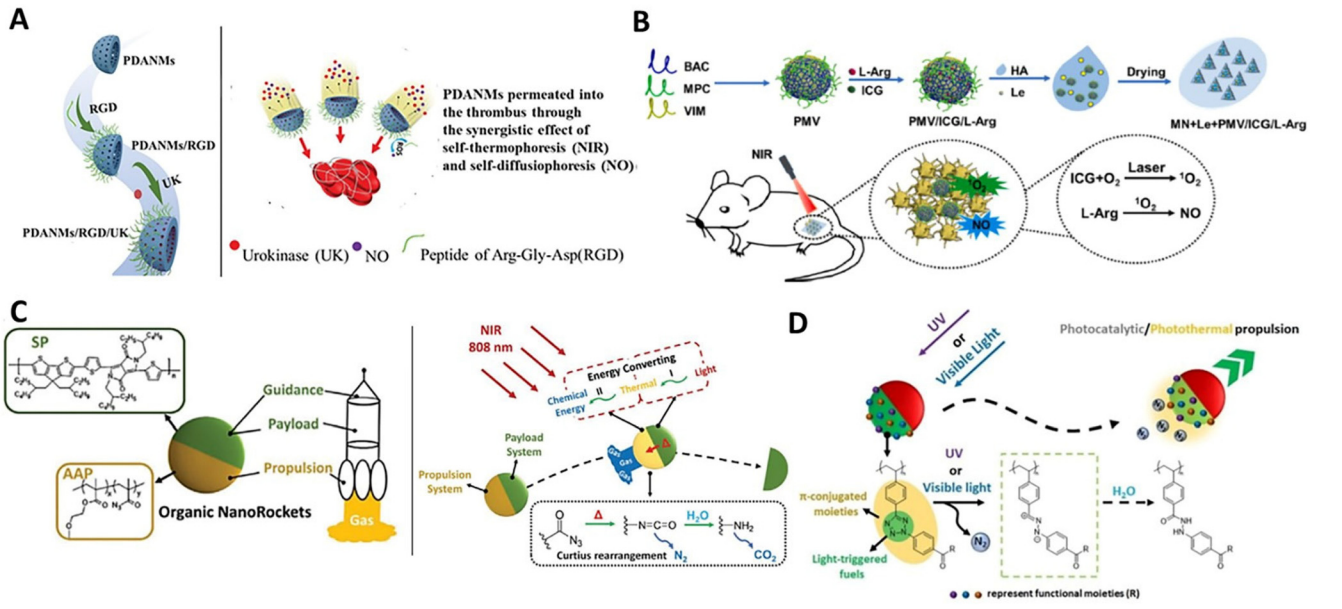

Fig. 5 Organic nanomotors with multi-mode kinetic systems. (A) Photothermal/chem-catalytic synergistic-driven nanomotors.[90] Reproduced from ref. 90 with permission from The Royal Society of Chemistry, copyright 2021. (B) Photothermal/chem-catalytic sequential-driven nanomotors.[91] Reproduced from ref. 91 with permission from Elsevier Ltd, copyright 2023. (C) Photothermal/thermos-catalytic sequential-driven nanomotors.[92] Reproduced from ref. 92 with permission from Wiley-VCH GmbH, copyright 2023. (D) Photothermal/photocatalytic synergistic-driven nanomotors.[94] Reproduced from ref. 94 with permission from Wiley-VCH GmbH, copyright 2023.

Published on 02 ianuarie 2024. Downloaded on 04.01.2026 05:56:20.

same orientation, so the different propelling forces exerted on the particles may induce a counterbalance between each other, resulting in a "seesaw effect" propulsion.[93] Recently, we fabricated photoactivated 105 nm-scaled organic colloidal motors with a single tetrazole-fueled engine for multimode synergistic propulsion (Fig. 5D).[94] In polymer chemistry, the tetrazole moieties are one of the important linkages capable of integrating the functionality to the polymers through a straight [3 + 2] cycloaddition,[95,96] which could further perform a photoactivated ring-opening reaction for bio-orthogonal ligation.[97,98] Also, the strong light-harvesting π-conjugated moieties endowed the polymer aggregates with photothermal converting capability. Thanks to the presence of tetrazole linkages, a sole light (ultraviolet or visible light) can simultaneously trigger photothermal conversion and photocatalytic nitrogen release within tetrazole-containing polymer phases. The spontaneous formation of thermal and chemical gradients with the same orientation would exert thermophoresis and diffusiophoresis force on the particles for powering photothermal/photocatalytic multimode synergistic propulsion in the aqueous solution. In the long-termed irradiation, the photothermal temperatures and N_2 production rates would vary with the consumption of tetrazole moieties. Also, the photodegradation rates also corresponded to light wavelengths (365, 405, and 450 nm) and laser powers (0–1000 mW cm^{-2}). Therefore, the particle velocities would evolve under irradiation (maximal: ~300 μm s^{-1}, 365 nm, 1000 mW cm^{-2}). Besides, various functionalities (biotin, fluoro groups, *etc.*) could be quantitatively incorporated into the particles *via* tetrazole linkages, which would effectively enlarge the application of nanomaterials in biomedical fields.

2.3.2. Photothermal/photoisomerization-driven organic nanomotors. In addition to intramolecular photoisomerization, liquid crystal azobenzene-bearing polymer aggregates also exhibit good photothermal converting capability, which has applicable prospects in various artificial intelligent devices.[99] Based on that, we applied a classic nanoprecipitation process to self-assemble azobenzene-bearing polymers and various macromolecular payloads (*e.g.*, PLA, polystyrene, and CPT-containing macromolecular prodrugs) into sub-200 nm-scaled Janus polymer nanomotors.[100] In contrast to surface grafting, the tight aggregation of azobenzene moieties within the particles can induce good photothermal conversion in response to 365 nm UV irradiation. In this case, the nanomotors simultaneously performed photoisomerization-induced internal mass migration and light-to-heat conversion for continuously converting light energy into mechanical motion. These behaviors highly corresponded to laser powers (365 nm, 0–500 mW cm^{-2}), particle morphologies (Janus *vs.* Plain), and payload rigidities (soft *vs.* rigid). Considering the motile mechanism, light-driven thermophoresis would be the main driving force, and photoisomerization-induced deformation can further facilitate particle locomotion.

2.4. Comparison with inorganic metal-based nanomotors

Organic fuels/engines have shown good performance in powering nanomotors, a brief comparison between organic and metal nanomotors is then provided here. Inorganic metal-based nanomotors have been exhaustively reviewed in recent years.[22,101,102] Metal-based nanomaterials have various interesting stimulus-responsive properties, such as electron transfer, electric polarization, plasma resonance, catalysis, and magnetism, which allows the metal-made nanomotors to carry out autonomous movement with a variety of mechanisms, including chemical, electric, thermophoretic, optical, and magnetic propulsion. In contrast, the so-far-developed organic nanomotors concentrate on several motile mechanisms. The organic fuels within the nanoparticles can perform a stimulus-responsive self-degradation for powering the particle transport, and some of them even can lead to self-dissociation of the nanomotors, which would be an attractive solution for relieving the common biosafety issues of engineered nanomaterials in biomedical applications. Meanwhile, light-driven organic engines can carry out various energy-conversion behaviors, but compared with metal nanoparticles with broadband strong light absorption, several organic nanomotors rely on a shorter wavelength of light (*i.e.*, UV) for the remote manipulation of their self-propelled motion, which may cause potential phototoxicity and restrict their bio-applications. The incorporation of upconversion luminescent system into the nanomotors for converting near-infrared light into short-wavelength light, or modulation of the optical properties of the organic molecules *via* structure modification for enlarging the absorbing range, both can improve the nanomotors to carry out the missions in a biosafe mode. In addition, in comparison with general nanofabrication techniques of metal-based nanomotors, the versatility of organic molecular assembly can achieve the controlled aggregation and ordered organization of various functional organic molecules within the nanoparticles for the programmable construction of multimode organic kinetic systems in a very convenient process. This would provide the high potential of on-demand reinforcement of the organic nanomotors.

3. The applications of organic nanomotors in antitumor therapy

Nanomedicines, due to their unique physicochemical features, have become potential therapeutics for antitumor therapy.[103,104] Some of them have achieved clinical transition.[105] However, the current nanomedicines in their passive delivery stage confront a series of biological obstacles in solid tumors, such as heterogeneous vascular networks, elevated interstitial fluid pressure (IFP), and dense extracellular matrix (ECM), which would seriously limit nanomedicines' tumor accumulation, tumor penetration, and accessibility to cancer cells, causing low delivery efficiency[106] and low antitumor efficacy.[107,108] In the past decades, many efforts have provided a series of significant contributions to the development of smart nanocarriers with stimulus-responsive physiochemical properties (such as size, shape, and surface-functionalization) for improving the diffusion at the tumor site.[109–111] In contrast to these nanocarriers highly dependent on blood flow, the

 This journal is © The Royal Society of Chemistry 2024

Published on 02 ianuarie 2024. Downloaded on 04.01.2026 05:56:20.

nanomotors with manipulatable self-propelled capability *in vitro* and *in vivo* can autonomously traverse various biological barriers to significantly enhance the adhesion, tumor penetration, and cellular internalization, resulting in the effective improvement of the therapeutic efficacy in antitumor therapy.[112–114] Recent studies have shown that organic nanomotors exhibit good performance on deep tumor penetration for significantly increasing the delivery efficiency to the solid tumor lesion. Meanwhile, the therapeutic chemicals produced by energy-converting organic reactions within the nanomotors can directly kill cancer cells and/or modulate the microenvironments to facilitate antitumor treatment.

3.1. Deep tumor penetration

The stimulus-responsive self-propelled delivery can endow the nanocarriers with high permeability against biological barriers in the solid tumor microenvironment, which would strongly promote the tumor accumulation, deep tumor penetration, and cellular uptake, achieving the directed delivery of therapeutic agents to the lesion with significantly enhanced efficiency.[10] Light has become more attractive external stimuli in antitumor treatment for its non-invasive, long-distance, and penetrative operations with finely tunable intensities and durations. Particularly, the nanomotors with photothermal converting kinetics achieve deep tumor penetration through surrounding medium-independent thermophoresis. Meanwhile, thermal production could lead to a significant increase in the temperature of the microenvironment, which would be used to ablate the cancer cells for hyperthermia.

The asymmetric nanomotors with azobenzene-bearing polymer-based engines showed good tumor penetration and cellular uptake *in vitro* (HepG2 cell culture and 3D MTS) and *in vivo* under irradiation of 365 nm UV light.[100] Thanks to the flexibility of polymer self-assembly, camptothecin-containing macromolecular prodrugs can be conveniently introduced into nanomotors as organic payloads. The enhanced transportability would significantly increase the drug delivery efficiency for improving the antitumor efficacy *in vitro* and *in vivo*. Taking advantage of a similar fabrication process, the similar group further developed asymmetric nanomotors with semiconducting conjugated polymer-based engines, which would achieve stable photothermal propulsion under more penetrative NIR irradiation.[83] Thanks to the NIR-activated delivery of anticancer prodrugs and simultaneous hyperthermia at 50 °C under long-term irradiation (5 min), such a synergetic photothermal/chemo-therapy would give rise to an obvious enhancement of antitumor efficacy. In addition, the manipulation advantage of light-driven nanomotors allowed for programming the locomotion in the microenvironment. Multiple start/stop *via* light on/off using short-term irradiation (2 min) for each time enabled the gradual improvement of the delivery efficiency and antitumor efficacy at a low dose and a low photothermal temperature (43 °C). This would effectively prevent non-specific damage of long-term hyperthermia to the surrounding health tissues.[115] Besides, thermoresponsive acyl azides were further incorporated into macromolecular anticancer prodrugs to fabricate the asymmetric nanomotors comprised of photothermal semiconducting conjugated polymer-based engines and thermoresponsive N_2 release propellants. NIR irradiation triggered a sequential two-stage light-to-heat-chemical energy transition, which endowed the nanomotors with enhanced self-propelled performance in the tumor microenvironment (Fig. 6A).[92] *In vitro* and *in vivo* results demonstrated that the photoactivated self-propulsion had good transportability crossing the tumor vascular membrane, extracellular tumor matrix, and cellular membrane for elevating tumor accumulation, deep penetration, and cellular uptake, resulting in the significant improvement of delivery efficiency of the prodrugs. The combined therapy of chemomedication and photothermal ablation led to the enhancement of the antitumor efficacy.

In addition, the polydopamine-powered nanomotors carrying anticancer doxorubicin in response to NIR irradiation can significantly increase the depth of the nanoparticles from 100 to 170 μm in MCF-7 three-dimensional multiple tumor spheroids (3D MTS).[85] The temperature increase simultaneously

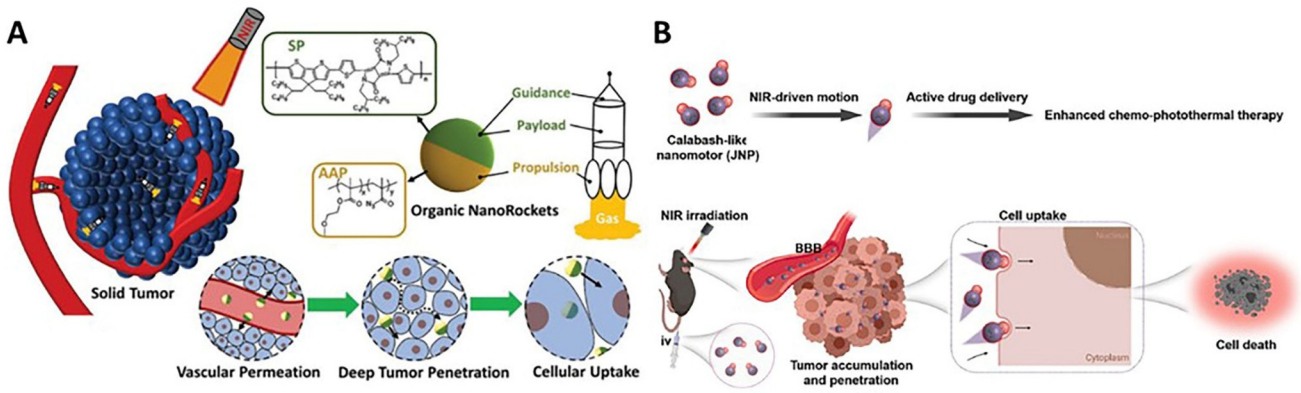

Fig. 6 Deep tumor penetration of (A) NIR-driven semiconducting conjugated polymer-powered organic nanomotors.[92] Reproduced from ref. 92 with permission from Wiley-VCH GmbH, copyright 2023. (B) NIR-driven ICG-powered organic nanomotors.[79] Reproduced from ref. 79 with permission from Elsevier Ltd, copyright 2023.

Published on 02 ianuarie 2024. Downloaded on 04.01.2026 05:56:20.

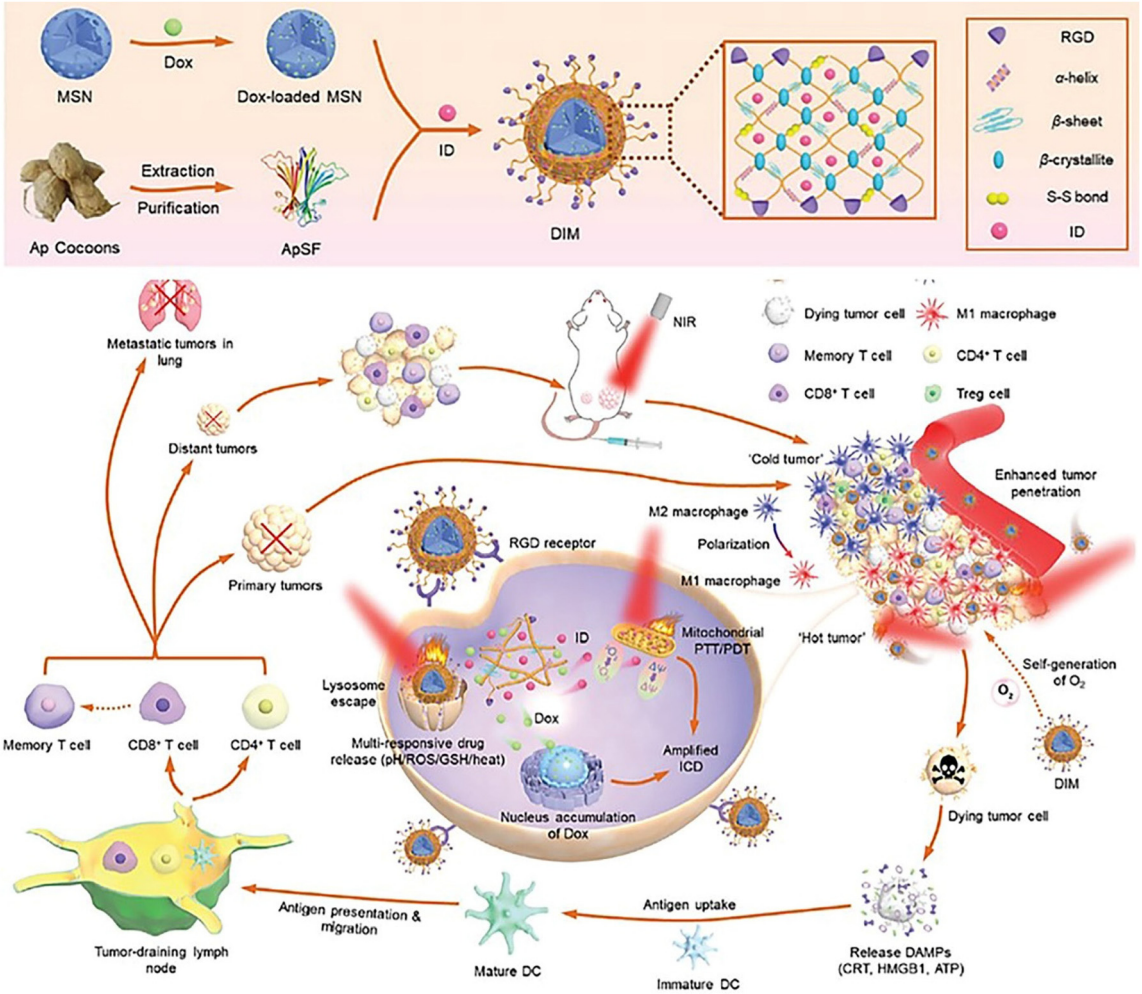

Fig. 7 Deep tumor penetration of NIR-driven multifunctional organic nanoplatforms.[80] Reproduced from ref. 80 with permission from Wiley-VCH GmbH, copyright 2022.

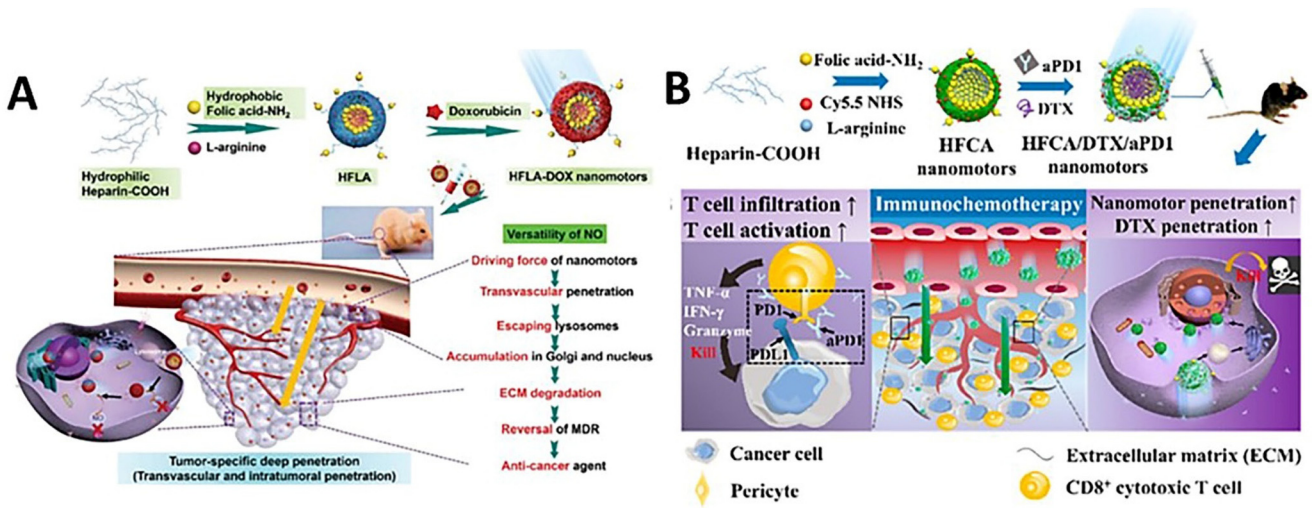

Fig. 8 Therapeutic performance of NO-driven nanomotors. (A) Versatility of NO-driven nanomotors for antitumor therapy.[49] Reproduced from ref. 49 with permission from Wiley-VCH GmbH, copyright 2021. (B) Mechanism of NO-driven nanomotors for regulating combined immunotherapy/chemotherapy for enhancing antitumor efficacy.[50] Reproduced from ref. 50 with permission from American Chemical Society, copyright 2021.

 This journal is © The Royal Society of Chemistry 2024

Published on 02 ianuarie 2024. Downloaded on 04.01.2026 05:56:20.

ablated the 3D MTS *via* a classic photothermal therapy. The light-driven motion effectively promoted the cellular internalization efficiency from 10.4 (NIR-free) to 19.4%. Also, doxorubicin-loaded Janus nanomotors with ICG-based engines could autonomously traverse the blood–brain barriers *via* NIR-driven propulsion (Fig. 6B).[79] With the reinforcement of transportability at the tumor site, the NIR-driven nanocarriers significantly increased the delivery efficiency *in vitro* (GL261 glioma cell culture and 3D MTS) and *in vivo* (glioblastoma). Photothermal conversion could initiate hyperthermia to further enhance the anti-glioma efficacy. The intelligent nanocarriers showed high potential antitumor applications in the central nervous system.

Nowadays, organic nanoparticles have been regarded as practical nanoplatforms integrating a large variety of diagnostic and therapeutic agents in antitumor therapy. Taking advantage of that, the arginine-glycine-aspartate (RGD) tripeptides, doxorubicin, and ICG derivatives can be straightforwardly incorporated into one organic particle to construct multi-functional organic nanomotors (Fig. 7).[80] NIR-triggered photothermal propulsion can force tumor-associated antigen penetration to facilitate the enhancement of doxorubicin delivery *in vitro* (4T1 cell culture and 3D MTS) and *in vivo* at the tumor site and to simultaneously activate systematic antitumor immunity against distant tumors. The triple modal treatment including photothermal, photodynamic, and chemotherapy can significantly enhance the efficacy against metastatic breast cancer.

3.2. Therapeutics

With the self-propulsion of the organic nanomotors in solid tumor tissue, degradable organic energy-converting components would act as consumable fuels to gradually release physiological signaling molecules to the surrounding tumor microenvironments *via* stimulus-responsive organic reactions. These bio-functional chemicals have shown good capabilities

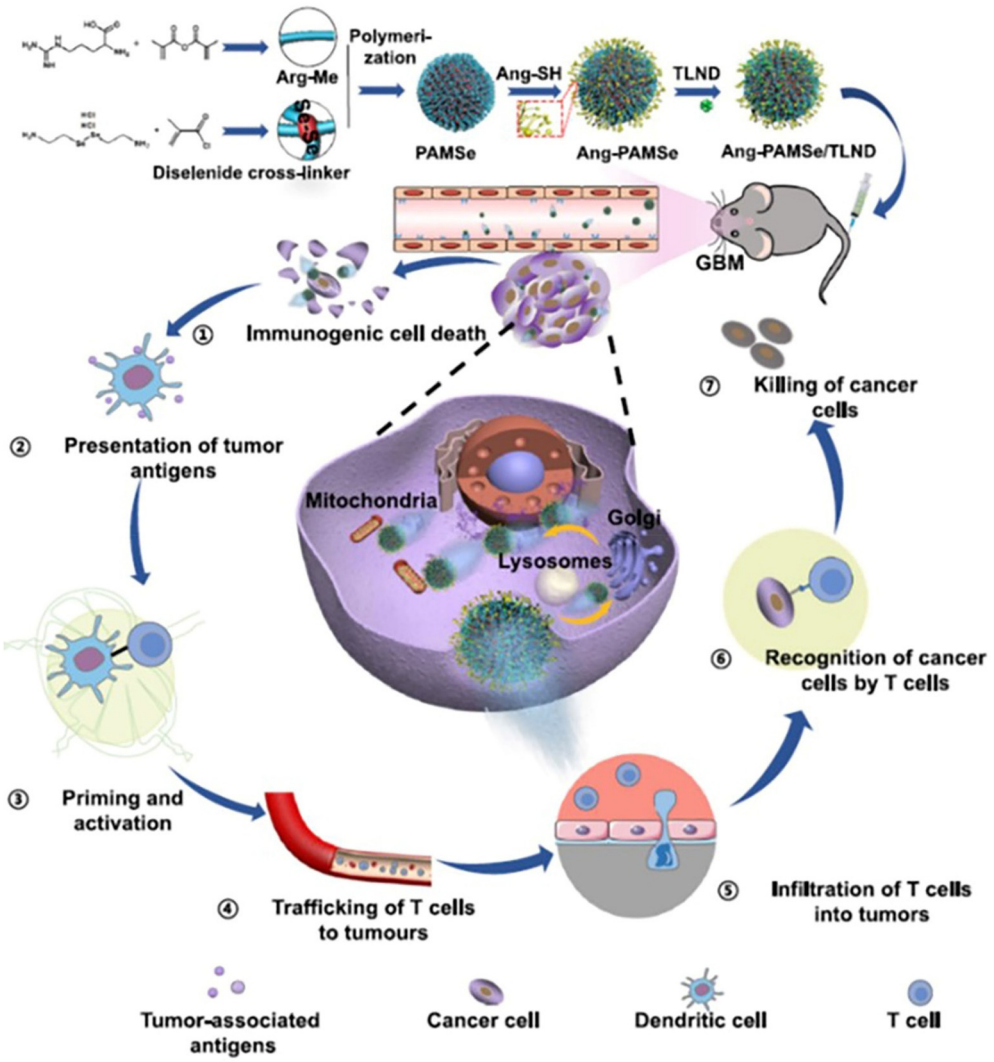

Fig. 9 Therapeutic performance of NO-driven nanomotors. Cascading effect of NO-driven nanomotors in enhanced immunotherapy against glioblastoma.[52] Reproduced from ref. 52 with permission from Springer Nature Limited, copyright 2023.

Published on 02 ianuarie 2024. Downloaded on 04.01.2026 05:56:20.

of regulating tumor microenvironments and/or immunogenic systems, which would effectively facilitate drug delivery in the microenvironment for improving the efficacy of chemotherapy and/or simultaneously trigger immunotherapy for achieving the combined therapeutic effect of immuno/chemotherapy.

NO can react with superoxide anions to form $ONOO^-$ in the tumor microenvironment, which could stimulate the generation of matrix metalloproteinases (MMPs) to degrade the collagen in the ECM.[116] In addition, NO can achieve the reversal of multidrug resistance in chemotherapy by inhibiting the overexpression of P-glycoprotein on cell membranes.[117] Based on this, catalytic NO production as a driving force of self-propulsion can also modulate the tumor microenvironments to promote vascular penetration, tumor penetration, and cellular uptake of doxorubicin-loaded nanoparticles *in vitro* (MCF-7/ADR cell culture and 3D MTS) and *in vivo*, improving the overall delivery efficiency.[49] Meanwhile, in addition to doxorubicin, highly concentrated NO can provide supplementary anticancer effects against cancer cells for enhancing the antitumor efficacy (Fig. 8A). In addition, NO release from the organic nanomotors during the drug delivery can normalize the tumor vasculature system for significantly improving T cell infiltration in the solid tumor.[50] The utilization of NO-driven nanomotors can achieve the combined therapeutic effect of immuno/chemotherapy for enhanced antitumor performance (Fig. 8B). A recent study showed that NO can play various vital roles in the modulation of the tumor microenvironment for facilitating immunotherapy. Specifically, NO production during chemotaxis can induce tumor immunogenic cell death, normalize tumor blood vessels, regulate matrix metalloproteinases, and macrophage polarization, and improve the selective inhibition of drug lonidamine derivatives on aerobic glycolysis and metabolism in tumor cells (Fig. 9).[52] The overall performance of NO cannot only efficiently promote the infiltration of T cells and carried drugs for increasing the delivery efficiency at the tumor site but also facilitate the drugs to destroy the tumor metabolic symbiosis for enhancing the antitumor efficacy. Hence, NO release with the self-propulsion of the organic nanomotors can be used as a very powerful therapeutic agent capable of achieving multistep intervention of brain tumor immune enhancement.

In addition, H_2S released from the colloidal motors can promote the cellular uptake of glucose in tumors, leading to the large production of lactic acid and effective inhibition of proton efflux, which would cause the acidosis of cancer cells.[63] Besides, a-cyano-4-hydroxycinnamic acid (a-CHCA) can be further loaded into H_2S-driven nanomotors. The presence of a-CHCA can inhibit the expression of MCT-1/4, which could cause the excessive accumulation of lactic acid in the cells for facilitating the acidosis of cancer cells, eventually inducing cell apoptosis efficiently (Fig. 10).

4. Conclusion and outlook

The review has summarized the recent advances in developing nanomotors with organic kinetic engines/fuels for stimulus-responsive self-propulsion in the aqueous solution or sophisticated biological environment. The versatility of stimulus-responsive behaviors of the organic molecules or aggregates provides a practical nanoscaled toolbox for programming the energy conversion within the nanomotors to reinforce the motile features and/or adapt to specific applications. The good biocompatibility and biodegradability of the organic kinetic systems allow an autonomously enhanced drug deliverability and therapeutic efficacy in a biosafe mode, suggesting the great potential of organic nanomotors in antitumor therapy.

Although organic nanomotors have exhibited appealing performance in practical applications, the research is still in the infancy stage. The progress in nanofabrication has allowed

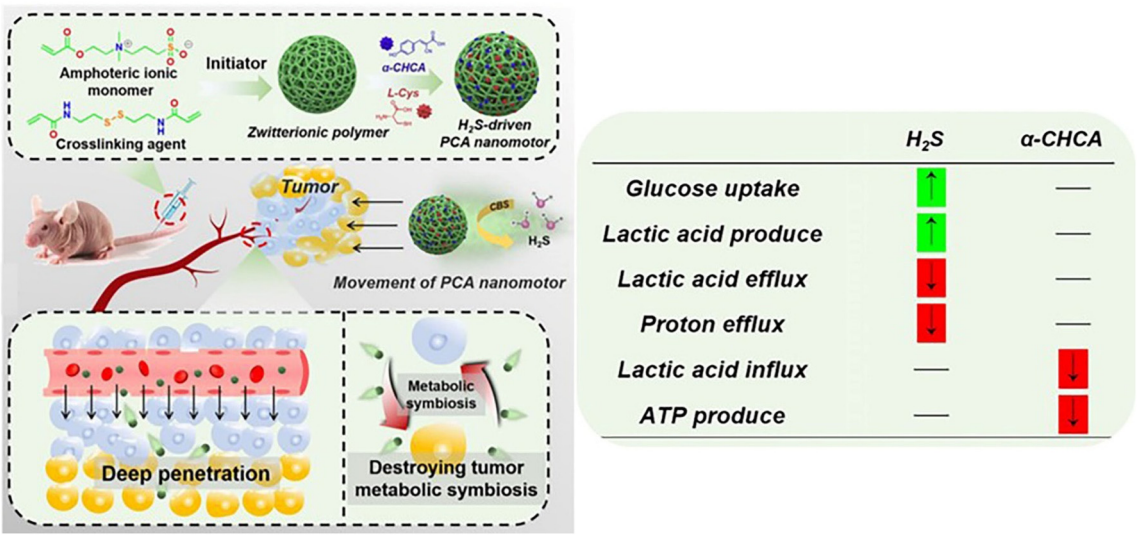

Fig. 10 Therapeutic performance of H_2S-driven nanomotors.[63] Reproduced from ref. 63 with permission from Wiley-VCH GmbH, copyright 2021.

 This journal is © The Royal Society of Chemistry 2024

Published on 02 ianuarie 2024. Downloaded on 04.01.2026 05:56:20.

the development of diverse organic kinetic systems with novel structures and compositions in the last years. However, for the aspect of mechanisms, the current stimulus-responsive autonomous movement concentrates on the photothermal- and catalytic-powered propulsion. The light-driven thermophoresis relies on light harvesting organic chromophores or aggregates for achieving a highly efficient light-to-heat transition. Except for converting photoenergy into thermal energy, a majority of organic chromophores have also exhibited other energy transfer behaviors under illumination with laser radiation, such as photochemical reaction, photodynamic process, and photoelectric effect. The exploration of the application potential of these energy-converting manners in powering mechanical motion with mono- or multi-mode mechanisms would be very attractive for developing versatile organic nanobots. In addition, for catalytic-powered organic nanomotors, current efforts are mainly devoted to enzyme-responsive organic fuels for driving self-propelled motion with high specificity in biological environments. However, these studies have received particular concerns for their high dependence on the surrounding biological mediums. The universality of these nanomotors should be considered for stable performance in complex tissues with inherent matter gradients. Compared with the progress in stimulus-responsive organic reactions in the last decades, the current catalytic-powered energy-converting behaviors are extremely limited. Hence, it is highly desired to achieve the construction of more diverse organic kinetic systems by introducing and programming these available reactions, which allows the production of more powerful nanomotors with practical application in universal or specific environments depending on the nature of the reactions.

Besides, material nanostructuration have shown a critical effect on their performance. However, the current investigations mostly rely on nanoparticles with very limited internal morphologies and shapes, which would restrict the exploration of their capability of finely regulating stimulus-responsive energy-converting processes and self-propelled motile behaviors. In stark contrast to metal-based nanoparticles, tremendous advances in organic molecular assembly at the nanoscale allow the controllable production of organic nanoparticles with much more complex internal nanostructures and shapes in very convenient processes.[118–120] This should require paying more attention to the design and synthesis of organic molecules with appropriate structures and physiochemical properties for achieving on-demand self-assembly into nanostructured organic nanomotors with more diversified energy conversion processes. These have not been developed yet and would be very interesting to explore their practical performance.

To summarize, artificial nanomotors with organic kinetic systems have shown their advantages in material fabrication and antitumor treatment. Particularly, the versatility of synthetic organic chemistry in molecular construction and energy transition provides convenient platforms for the integration and programming of various energy-converting modes within the nanomotors. With more in-depth research, we believe that there would be an appealing prospect for organic nanomotors with diversified organic kinetic systems in biomedical applications.

Conflicts of interest

There are no conflicts to declare.

Acknowledgements

We thank the financial support from the National Natural Science Foundation of China (21902117), the Natural Science Foundation of Tianjin (20JCQNJC01110) and the Open Project of China Food Flavor and Nutrition Health Innovation Center (CFC2023B-002).

References

1 Y. Hong, N. M. K. Blackman, N. D. Kopp, A. Sen and D. Velegol, *Phys. Rev. Lett.*, 2007, **99**, 178103.
2 L. Xu, F. Mou, H. Gong, M. Luo and J. Guan, *Chem. Soc. Rev.*, 2017, **46**, 6905–6926.
3 T. Xu, L.-P. Xu and X. Zhang, *Appl. Mater. Today*, 2017, **9**, 493–503.
4 H. Zhou, C. C. Mayorga-Martinez, S. Pané, L. Zhang and M. Pumera, *Chem. Rev.*, 2021, **121**, 4999–5041.
5 F. Novotný, H. Wang and M. Pumera, *Chem*, 2020, **6**, 867–884.
6 J. Wang, *ACS Nano*, 2009, **3**, 4–9.
7 S. Sengupta, M. E. Ibele and A. Sen, *Angew. Chem., Int. Ed.*, 2012, **51**, 8434–8445.
8 M. Luo, Y. Feng, T. Wang and J. Guan, *Adv. Funct. Mater.*, 2018, **28**, 1706100.
9 S. Campuzano, D. Kagan, J. Orozco and J. Wang, *Analyst*, 2011, **136**, 4621–4630.
10 C. Gao, Y. Wang, Z. Ye, Z. Lin, X. Ma and Q. He, *Adv. Mater.*, 2021, **33**, 2000512.
11 W. Gao and J. Wang, *ACS Nano*, 2014, **8**, 3170–3180.
12 K. Villa and M. Pumera, *Chem. Soc. Rev.*, 2019, **48**, 4966–4978.
13 C. Chen, F. Soto, E. Karshalev, J. Li and J. Wang, *Adv. Funct. Mater.*, 2019, **29**, 1806290.
14 Y. Ye, J. Luan, M. Wang, Y. Chen, D. A. Wilson, F. Peng and Y. Tu, *Chem. – Eur. J.*, 2019, **25**, 8663–8680.
15 F. Zha, T. Wang, M. Luo and J. Guan, *Micromachines*, 2018, **9**, 78.
16 G. Loget, D. Zigah, L. Bouffier, N. Sojic and A. Kuhn, *Acc. Chem. Res.*, 2013, **46**, 2513–2523.
17 M. Yan, K. Liang, D. Zhao and B. Kong, *Small*, 2022, **18**, 2102887.
18 Y. Tu, F. Peng and D. A. Wilson, *Adv. Mater.*, 2017, **29**, 1701970.
19 L. Shao and M. Käll, *Adv. Funct. Mater.*, 2018, **28**, 1706272.

Published on 02 ianuarie 2024. Downloaded on 04.01.2026 05:56:20.

20 W. Z. Teo and M. Pumera, *Chem. – Eur. J.*, 2016, **22**, 14796–14804.
21 W. F. Paxton, K. C. Kistler, C. C. Olmeda, A. Sen, S. K. St. Angelo, Y. Cao, T. E. Mallouk, P. E. Lammert and V. H. Crespi, *J. Am. Chem. Soc.*, 2004, **126**, 13424–13431.
22 H. Šípová-Jungová, D. Andrén, S. Jones and M. Käll, *Chem. Rev.*, 2020, **120**, 269–287.
23 S. Cao, J. Shao, H. Wu, S. Song, M. T. De Martino, I. A. B. Pijpers, H. Friedrich, L. K. E. A. Abdelmohsen, D. S. Williams and J. C. M. van Hest, *Nat. Commun.*, 2021, **12**, 2077.
24 L. Yue, K. Yang, J. Li, Q. Cheng and R. Wang, *Small*, 2021, **17**, 2102286.
25 F. Peng, Y. Tu and D. A. Wilson, *Chem. Soc. Rev.*, 2017, **46**, 5289–5310.
26 E. Miyako, J. Russier, M. Mauro, C. Cebrian, H. Yawo, C. Ménard-Moyon, J. A. Hutchison, M. Yudasaka, S. Iijima, L. De Cola and A. Bianco, *Angew. Chem., Int. Ed.*, 2014, **53**, 13121–13125.
27 H. Nakatsuji, T. Numata, N. Morone, S. Kaneko, Y. Mori, H. Imahori and T. Murakami, *Angew. Chem., Int. Ed.*, 2015, **54**, 11725–11729.
28 H.-J. Yen, S.-h. Hsu and C.-L. Tsai, *Small*, 2009, **5**, 1553–1561.
29 D. Fu, Z. Wang, Y. Tu and F. Peng, *Adv. Healthcare Mater.*, 2021, **10**, 2001788.
30 M. Horie and K. Fujita, in *Advances in Molecular Toxicology*, ed. J. C. Fishbein, Elsevier, 2011, vol. 5, pp. 145–178.
31 N. Kamaly, Z. Xiao, P. M. Valencia, A. F. Radovic-Moreno and O. C. Farokhzad, *Chem. Soc. Rev.*, 2012, **41**, 2971–3010.
32 J. Ou, K. Liu, J. Jiang, D. A. Wilson, L. Liu, F. Wang, S. Wang, Y. Tu and F. Peng, *Small*, 2020, **16**, 1906184.
33 H. Wang and M. Pumera, *Chem. Rev.*, 2015, **115**, 8704–8735.
34 X. Ma, A. C. Hortelão, T. Patiño and S. Sánchez, *ACS Nano*, 2016, **10**, 9111–9122.
35 M. Mathesh, J. Sun and D. A. Wilson, *J. Mater. Chem. B*, 2020, **8**, 7319–7334.
36 X. Arqué, T. Patiño and S. Sánchez, *Chem. Sci.*, 2022, **13**, 9128–9146.
37 H. Yuan, X. Liu, L. Wang and X. Ma, *Bioact. Mater.*, 2021, **6**, 1727–1749.
38 H. Mutlu, C. M. Geiselhart and C. Barner-Kowollik, *Mater. Horiz.*, 2018, **5**, 162–183.
39 M. A. Ayer, Y. C. Simon and C. Weder, *Macromolecules*, 2016, **49**, 2917–2927.
40 S. Jiang, A. Kaltbeitzel, M. Hu, O. Suraeva, D. Crespy and K. Landfester, *ACS Nano*, 2020, **14**, 498–508.
41 A. Feng, X. Huang, X. Cheng, M. Chu, S. Wang and X. Yan, *Chem. Eng. J.*, 2022, **440**, 135838.
42 R. M. J. Palmer, A. G. Ferrige and S. Moncada, *Nature*, 1987, **327**, 524–526.
43 L. J. Ignarro, *Biochem. Pharmacol.*, 1991, **41**, 485–490.
44 G. Wu and S. M. Morris Jr., *Biochem. J.*, 1998, **336**, 1–17.
45 S. Moncada and A. Higgs, *N. Engl. J. Med.*, 1993, **329**, 2002–2012.
46 M. Wan, H. Chen, Q. Wang, Q. Niu, P. Xu, Y. Yu, T. Zhu, C. Mao and J. Shen, *Nat. Commun.*, 2019, **10**, 966.
47 Y. Tao, X. Li, Z. Wu, C. Chen, K. Tan, M. Wan, M. Zhou and C. Mao, *J. Colloid Interface Sci.*, 2022, **611**, 61–70.
48 T. Li, Z. Liu, J. Hu, L. Chen, T. Chen, Q. Tang, B. Yu, B. Zhao, C. Mao and M. Wan, *Adv. Mater.*, 2022, **34**, 2206654.
49 M. M. Wan, H. Chen, Z. Da Wang, Z. Y. Liu, Y. Q. Yu, L. Li, Z. Y. Miao, X. W. Wang, Q. Wang, C. Mao, J. Shen and J. Wei, *Adv. Sci.*, 2021, **8**, 2002525.
50 H. Chen, T. Shi, Y. Wang, Z. Liu, F. Liu, H. Zhang, X. Wang, Z. Miao, B. Liu, M. Wan, C. Mao and J. Wei, *J. Am. Chem. Soc.*, 2021, **143**, 12025–12037.
51 Q. Wang, T. Li, J. Yang, Z. Zhao, K. Tan, S. Tang, M. Wan and C. Mao, *Adv. Mater.*, 2022, **34**, 2201406.
52 H. Chen, T. Li, Z. Liu, S. Tang, J. Tong, Y. Tao, Z. Zhao, N. Li, C. Mao, J. Shen and M. Wan, *Nat. Commun.*, 2023, **14**, 941.
53 X. Tang, L. Chen, Z. Wu, Y. Li, J. Zeng, W. Jiang, W. Lv, M. Wan, C. Mao and M. Zhou, *Small*, 2023, **19**, 2203238.
54 Z. Wu, M. Zhou, X. Tang, J. Zeng, Y. Li, Y. Sun, J. Huang, L. Chen, M. Wan and C. Mao, *ACS Nano*, 2022, **16**, 3808–3820.
55 P. G. Wang, M. Xian, X. Tang, X. Wu, Z. Wen, T. Cai and A. J. Janczuk, *Chem. Rev.*, 2002, **102**, 1091–1134.
56 L. J. Ignarro, C. Napoli and J. Loscalzo, *Circ. Res.*, 2002, **90**, 21–28.
57 Z. Huang, J. Fu and Y. Zhang, *J. Med. Chem.*, 2017, **60**, 7617–7635.
58 J. E. Keeble and P. K. Moore, *Br. J. Pharmacol.*, 2002, **137**, 295–310.
59 J. Peng, S. Xie, K. Huang, P. Ran, J. Wei, Z. Zhang and X. Li, *J. Mater. Chem. B*, 2022, **10**, 4189–4202.
60 J. Li, X. Li, Y. Yuan, Q. Wang, L. Xie, Y. Dai, W. Wang, L. Li, X. Lu, Q. Fan and W. Huang, *Small*, 2020, **16**, 2002939.
61 Z.-W. Lee, X.-Y. Teo, E. Y.-W. Tay, C.-H. Tan, T. Hagen, P. K. Moore and L.-W. Deng, *Br. J. Pharmacol.*, 2014, **171**, 4322–4336.
62 X. Cao, L. Ding, Z.-z. Xie, Y. Yang, M. Whiteman, P. K. Moore and J.-S. Bian, *Antioxid. Redox Signaling*, 2019, **31**, 1–38.
63 M. Wan, Z. Liu, T. Li, H. Chen, Q. Wang, T. Chen, Y. Tao and C. Mao, *Angew. Chem., Int. Ed.*, 2021, **60**, 16139–16148.
64 L. Li, M. Whiteman, Y. Y. Guan, K. L. Neo, Y. Cheng, S. W. Lee, Y. Zhao, R. Baskar, C.-H. Tan and P. K. Moore, *Circulation*, 2008, **117**, 2351–2360.
65 F. Tong, J. Liu, L. Luo, L. Qiao, J. Wu, G. Wu and Q. Mei, *Nanoscale*, 2023, **15**, 6745–6758.
66 F. Ercole, T. P. Davis and R. A. Evans, *Polym. Chem.*, 2010, **1**, 37–54.
67 N. Katsonis, M. Lubomska, M. M. Pollard, B. L. Feringa and P. Rudolf, *Prog. Surf. Sci.*, 2007, **82**, 407–434.

 This journal is © The Royal Society of Chemistry 2024

Published on 02 ianuarie 2024. Downloaded on 04.01.2026 05:56:20.

68 A. Kausar, H. Nagano, T. Ogata, T. Nonaka and S. Kurihara, *Angew. Chem., Int. Ed.*, 2009, **48**, 2144–2147.
69 S. Loebner, J. Jelken, N. S. Yadavalli, E. Sava, N. Hurduc and S. Santer, *Molecules*, 2016, **21**, 1663.
70 Y. Tu, F. Peng, J. M. Heuvelmans, S. Liu, R. J. M. Nolte and D. A. Wilson, *Angew. Chem., Int. Ed.*, 2019, **58**, 8687–8691.
71 Z. Ye, Y. Wang, S. Liu, D. Xu, W. Wang and X. Ma, *J. Am. Chem. Soc.*, 2021, **143**, 15063–15072.
72 J.-P. Abid, M. Frigoli, R. Pansu, J. Szeftel, J. Zyss, C. Larpent and S. Brasselet, *Langmuir*, 2011, **27**, 7967–7971.
73 W. Li, X. Wu, H. Qin, Z. Zhao and H. Liu, *Adv. Funct. Mater.*, 2016, **26**, 3164–3171.
74 H.-R. Jiang, N. Yoshinaga and M. Sano, *Phys. Rev. Lett.*, 2010, **105**, 268302.
75 A. O. Govorov and H. H. Richardson, *Nano Today*, 2007, **2**, 30–38.
76 L. Xu, L. Cheng, C. Wang, R. Peng and Z. Liu, *Polym. Chem.*, 2014, **5**, 1573–1580.
77 P.-Y. Xu, X. Zheng, R. K. Kankala, S.-B. Wang and A.-Z. Chen, *ACS Biomater. Sci. Eng.*, 2021, **7**, 939–962.
78 E. P. Porcu, A. Salis, E. Gavini, G. Rassu, M. Maestri and P. Giunchedi, *Biotechnol. Adv.*, 2016, **34**, 768–789.
79 H. Li, X. Zhang, J. Miao, Z. Shi, Z. Li, M. Wen, L. Wang, J. Liang, J. Gao, Y. Ye, H. Tian, F. Peng and Y. Tu, *Chem. Eng. J.*, 2023, **473**, 145413.
80 X. Zhang, Q. He, J. Sun, H. Gong, Y. Cao, L. Duan, S. Yi, B. Ying and B. Xiao, *Adv. Healthcare Mater.*, 2022, **11**, 2200255.
81 J. Li and K. Pu, *Acc. Chem. Res.*, 2020, **53**, 752–762.
82 Y. Jiang and K. Pu, *Acc. Chem. Res.*, 2018, **51**, 1840–1849.
83 X. Huang, Y. Liu, A. Feng, X. Cheng, X. Xiong, Z. Wang, Z. He, J. Guo, S. Wang and X. Yan, *Small*, 2022, **18**, 2201525.
84 Y. Liu, K. Ai and L. Lu, *Chem. Rev.*, 2014, **114**, 5057–5115.
85 Y. Liu, Y. Zhang, J. Wang, H. Yang, J. Zhou and W. Zhao, *Bioconjugate Chem.*, 2022, **33**, 726–735.
86 M. Wu, S. Liu, Z. Liu, F. Huang, X. Xu and Q. Shuai, *Colloids Surf., B*, 2022, **212**, 112353.
87 S. Feng, J. Lu, K. Wang, D. Di, Z. Shi, Q. Zhao and S. Wang, *Chem. Eng. J.*, 2022, **435**, 134886.
88 L. Xie, M. Yan, T. Liu, K. Gong, X. Luo, B. Qiu, J. Zeng, Q. Liang, S. Zhou, Y. He, W. Zhang, Y. Jiang, Y. Yu, J. Tang, K. Liang, D. Zhao and B. Kong, *J. Am. Chem. Soc.*, 2022, **144**, 1634–1646.
89 Z. Wu, R. Wu, X. Li, X. Wang, X. Tang, K. Tan, M. Wan, C. Mao, X. Xu, H. Jiang, J. Li, M. Zhou and D. Shi, *Small*, 2022, **18**, 2104120.
90 D. Fang, T. Li, Z. Wu, Q. Wang, M. Wan, M. Zhou and C. Mao, *J. Mater. Chem. B*, 2021, **9**, 8659–8666.
91 L. Chen, D. Fang, J. Zhang, X. Xiao, N. Li, Y. Li, M. Wan and C. Mao, *J. Colloid Interface Sci.*, 2023, **647**, 142–151.
92 A. Feng, X. Cheng, X. Huang, Y. Liu, Z. He, J. Zhao, H. Duan, Z. Shi, J. Guo, S. Wang and X. Yan, *Small*, 2023, **19**, 2206426.
93 J. Shao, S. Cao, H. Che, M. T. De Martino, H. Wu, L. K. E. A. Abdelmohsen and J. C. M. van Hest, *J. Am. Chem. Soc.*, 2022, **144**, 11246–11252.
94 J. Jin, Y. Li, D. Cao, S. Wang and X. Yan, *Angew. Chem., Int. Ed.*, 2023, **62**, e202306169.
95 H. Zhao, Z.-R. Qu, H.-Y. Ye and R.-G. Xiong, *Chem. Soc. Rev.*, 2008, **37**, 84–100.
96 F. Himo, Z. P. Demko, L. Noodleman and K. B. Sharpless, *J. Am. Chem. Soc.*, 2002, **124**, 12210–12216.
97 J. Hatano, K. Okuro and T. Aida, *Angew. Chem., Int. Ed.*, 2016, **55**, 193–198.
98 R. Müller, T. J. Feuerstein, V. Trouillet, S. Bestgen, P. W. Roesky and C. Barner-Kowollik, *Chem. – Eur. J.*, 2018, **24**, 18933–18943.
99 L. Dong and Y. Zhao, *Mater. Chem. Front.*, 2018, **2**, 1932–1943.
100 X. Xiong, X. Huang, Y. Liu, A. Feng, Z. Wang, X. Cheng, Z. He, S. Wang, J. Guo and X. Yan, *Chem. Eng. J.*, 2022, **445**, 136576.
101 H. Zhao, Y. Zheng, Y. Cai, T. Xu, R. Dong and X. Zhang, *Nano Today*, 2023, **52**, 101939.
102 K. Kim, J. Guo, X. Xu and D. L. Fan, *Small*, 2015, **11**, 4037–4057.
103 J. Shi, P. W. Kantoff, R. Wooster and O. C. Farokhzad, *Nat. Rev. Cancer*, 2017, **17**, 20–37.
104 M. E. Davis, Z. Chen and D. M. Shin, *Nat. Rev. Drug Discovery*, 2008, **7**, 771–782.
105 A. Akinc, M. A. Maier, M. Manoharan, K. Fitzgerald, M. Jayaraman, S. Barros, S. Ansell, X. Du, M. J. Hope, T. D. Madden, B. L. Mui, S. C. Semple, Y. K. Tam, M. Ciufolini, D. Witzigmann, J. A. Kulkarni, R. van der Meel and P. R. Cullis, *Nat. Nanotechnol.*, 2019, **14**, 1084–1087.
106 *Nat. Nanotechnol.*, 2019, **14**, 1083–1083.
107 A. I. Minchinton and I. F. Tannock, *Nat. Rev. Cancer*, 2006, **6**, 583–592.
108 J. L. S. Au, B. Z. Yeung, M. G. Wientjes, Z. Lu and M. G. Wientjes, *Adv. Drug Delivery Rev.*, 2016, **97**, 280–301.
109 G. Cheng, D. Wu, S. Wang, X. Zhang, P. Yu, J. Chang and X. Chen, *Nano Today*, 2021, **38**, 101208.
110 Z. Zhang, H. Wang, T. Tan, J. Li, Z. Wang and Y. Li, *Adv. Funct. Mater.*, 2018, **28**, 1801840.
111 Z. Li, X. Shan, Z. Chen, N. Gao, W. Zeng, X. Zeng and L. Mei, *Adv. Sci.*, 2021, **8**, 2002589.
112 J. Wang, R. Dong, H. Wu, Y. Cai and B. Ren, *Nano-Micro Lett.*, 2019, **12**, 11.
113 A. H. Meisami, M. Abbasi, S. Mosleh-Shirazi, A. Azari, A. M. Amani, A. Vaez and A. Golchin, *Eur. J. Pharmacol.*, 2022, **926**, 175011.
114 T. Li, M. Wan and C. Mao, *ChemPlusChem*, 2020, **85**, 2586–2598.
115 D. Jaque, L. M. Maestro, B. del Rosal, P. Haro-Gonzalez, A. Benayas, J. L. Plaza, E. M. Rodríguez and J. G. Solé, *Nanoscale*, 2014, **6**, 9494–9530.
116 X. Dong, H.-J. Liu, H.-Y. Feng, S.-C. Yang, X.-L. Liu, X. Lai, Q. Lu, J. F. Lovell, H.-Z. Chen and C. Fang, *Nano Lett.*, 2019, **19**, 997–1008.

117 A. Alam, J. Kowal, E. Broude, I. Roninson and K. P. Locher, *Science*, 2019, **363**, 753–756.
118 T. L. Kelly and M. O. Wolf, *Chem. Soc. Rev.*, 2010, **39**, 1526–1535.
119 R. Deng, J. Xu, G.-R. Yi, J. W. Kim and J. Zhu, *Adv. Funct. Mater.*, 2021, **31**, 2008169.
120 X. Yan, J. Bernard and F. Ganachaud, *Adv. Colloid Interface Sci.*, 2021, **294**, 102474.

Published on 02 ianuarie 2024. Downloaded on 04.01.2026 05:56:20.

This journal is © The Royal Society of Chemistry 2024